AoB PLANTS 2020, Vol. 12, No. 6

doi:10.1093/aobpla/plaa058
Advance Access Publication November 13, 2020
Studies

STUDIES

Convergent patterns of tissue-level distribution of elements in different tropical woody nickel hyperaccumulator species from Borneo Island

Farida Abubakari[1], Jolanta Mesjasz-Przybyłowicz[2], Wojciech J. Przybyłowicz[2,3] and Antony van der Ent[1,4*]

[1]Centre for Mined Land Rehabilitation, Sustainable Minerals Institute, The University of Queensland, Sir James Foots Building, Brisbane, QLD 4072, Australia, [2]Department of Botany and Zoology, Stellenbosch University, Private Bag X1, Matieland 7602, South Africa, [3]AGH University of Science and Technology, Faculty of Physics & Applied Computer Science, al. Mickiewicza 30, 30-059 Kraków, Poland, [4]Universite de Lorraine – INRA, Laboratoire Sols et Environnement, UMR 1120, F-54505 Vandoeuvre-les-Nancy, France

*Corresponding author's e-mail address: a.vanderent@uq.edu.au

Form & Function. Chief Editor: Kate McCulloh

Associate Editor: Nishanta Rajakaruna

Abstract

The Malaysian state of Sabah on the Island of Borneo has recently emerged as a global hotspot of nickel hyperaccumulator plants. This study focuses on the tissue-level distribution of nickel and other physiologically relevant elements in hyperaccumulator plants with distinct phylogenetical affinities. The roots, old stems, young stems and leaves of *Flacourtia kinabaluensis* (Salicaceae), *Actephila alanbakeri* (Phyllanthaceae), *Psychotria sarmentosa* (Rubiaceae) and young stems and leaves of *Glochidion brunneum* (Phyllanthaceae) were studied using nuclear microprobe (micro-PIXE and micro-BS) analysis. The tissue-level distribution of nickel found in these species has the same overall pattern as in most other hyperaccumulator plants studied previously, with substantial enrichment in the epidermal cells and in the phloem. This study also revealed enrichment of potassium in the spongy and palisade mesophyll of the studied species. Calcium, chlorine, manganese and cobalt were found to be enriched in the phloem and also concentrated in the epidermis and cortex of the studied species. Although hyperaccumulation ostensibly evolved numerous times independently, the basic mechanisms inferred from tissue elemental localization are convergent in these tropical woody species from Borneo Island.

Keywords: Elemental distribution; elemental maps; hyperaccumulator; micro-PIXE; nuclear microprobe; X-ray microanalysis.

Introduction

Plants require some trace elements in minor quantities (e.g. Mn, Fe, Ni, Zn) for healthy growth, whereas excess of these can lead to toxicity symptoms (DalCorso *et al.* 2014). Other elements, such as Na, Al, Si and Co, although not essential, are known to be beneficial to some plant species (Pilon-Smits *et al.* 2009). Macronutrients (Mg, P, S, K and Ca) are needed for basic plant metabolism and to protect plants from various abiotic and biotic stresses (Shanker and Venkateswarlu 2011; Rowley *et al.* 2012; Morgan and Connolly 2013). Hyperaccumulators are plants that accumulate trace elements to extreme concentrations (e.g. Ni > 1000 μg g^{-1}) in their living shoots (Reeves 2003; van der Ent *et al.* 2013a). There are currently >500 nickel hyperaccumulator plant

Received: 10 June 2020; **Editorial decision:** 29 October 2020; **Accepted:** 10 November 2020

species known globally, with the greatest number of species recorded in Cuba, New Caledonia and the Mediterranean Region (Baker and Brooks 1988; Reeves 2003; Reeves *et al.* 2017). At a global scale, the most common families of Ni hyperaccumulators in tropical regions are the Phyllanthaceae, Rubiaceae and Salicaceae (Reeves 2006). Nickel hyperaccumulator plants have the potential to be used in phytomining, an environmentally sustainable 'green' technology to produce Ni (Chaney 1983; Chaney *et al.* 1998, 2007; van der Ent *et al.* 2013b). In a phytomining operation, hyperaccumulator plants are grown on ultramafic soils, followed by harvesting, drying and incineration of the above-ground biomass to generate a commercial high-grade Ni bio-ore (Brooks and Robinson 1998; Chaney *et al.* 2007, 2018; van der Ent *et al.* 2013b, 2017c; Bani *et al.* 2015).

The ultramafic soils of the Malaysian state of Sabah on the Island of Borneo are renowned for high species richness (van der Ent *et al.* 2014), with over 5000 plant species known from the <1200 km^2 Kinabalu Park area (Beaman 2005) and 2854 plant species in 742 genera and 188 families recorded from the ultramafic soils in Kinabalu Park (van der Ent *et al.* 2014, 2016). In Sabah, 28 Ni hyperaccumulator species in 10 families and 17 genera are now known (van der Ent *et al.* 2019b), and most Ni hyperaccumulator species are from the order Malpighiales, predominantly in the families Phyllanthaceae, Salicaceae and Violaceae (van der Ent *et al.* 2019a, b).

Actephila alanbakeri and *Glochidion brunneum* (Fig. 1) are both members of the Phyllanthaceae family, which globally has the greatest numbers of Ni hyperaccumulating taxa (Reeves 2003) together with the closely related families Buxaceae (genus: *Buxus*) and Euphorbiaceae (genus: *Leucocroton*). *Glochidion brunneum* is widespread in Indonesia, Malaysia and the Philippines. In contrast, *A. alanbakeri* is a local endemic known from just two populations in Sabah near Kinabalu Park and Malawali Island. *Glochidion brunneum* is a medium-sized (up to 10 m tall) understorey tree of lowland rainforest. It can accumulate up to 6200 µg g^{-1} foliar Ni (van der Ent *et al.* 2015a). *Actephila alanbakeri* is a small (up to 3 m tall) woody shrub of disturbed habitats on eroded soils (Hypermagnesian Cambisols). This species may accumulate up to 14 700 µg g^{-1} foliar Ni (van der Ent *et al.* 2015b). *Psychotria sarmentosa* is a member of Rubiaceae family (Fig. 1) and is a climber that occurs in lowland forest, mainly in disturbed areas. The species is widespread in Indonesia, Malaysia and the Philippines. It is a strong Ni hyperaccumulator which can attain up to 24 200 µg g^{-1} foliar Ni (van der Ent *et al.* 2015a) (Fig. 1). *Flacourtia kinabaluensis* is a member of the Salicaceae family. It is a small tree (up to 8–12 m tall) that primarily occurs in riparian habitats. This species is a local endemic of the Kinabalu Park region of Sabah, Malaysia. It accumulates up to 7300 foliar µg g^{-1} Ni (van der Ent *et al.* 2015a) (Fig. 1).

Previous studies regarding the distribution and chemical speciation of Ni in hyperaccumulators from Borneo (Sabah) have focussed on *Rinorea* cf. *bengalensis*, *R.* cf. *javanica* (Violaceae), *Phyllanthus balgooyi*, *P. rufuschaneyi* (previously designated as *P.* cf. *securinegoides*) and *Glochidion* cf. *sericeum* (Phyllanthaceae) using nuclear microprobe (micro-proton-induced X-ray emission (micro-PIXE)) analysis with backscattering spectrometry (BS). Additionally, Ni distribution in these species has been studied with the use of synchrotron X-ray Fluorescence Microscopy (XFM) and X-ray Absorption Spectroscopy (XAS) techniques (Mesjasz-Przybyłowicz *et al.* 2016a; van der Ent *et al.* 2017a, 2018, 2020). The results showed that Ni was primarily concentrated in the epidermal areas of the leaves, and Ni in roots and stems of all three species was exceptionally enriched in the phloem. Nickel distribution in leaves, however, varies by species. In *P. balgooyi* the highest foliar Ni concentration was in the phloem, but in *P. rufuschaneyi* and *R. bengalensis* the highest foliar Ni concentration was in the epidermis and spongy mesophyll (*R.* cf. *bengalensis*). *Phyllanthus balgooyi* was unusual with extreme

Figure 1. Foliage of the Ni hyperaccumulator plants species studied. (A) *Actephila alanbakeri*, (B) *Glochidion brunneum*, (C) *Psychotria sarmentosa* and (D) *Flacourtia kinabaluensis*.

accumulation of Ni in the phloem with up to 169 g kg^{-1} Ni in the phloem sap (van der Ent and Mulligan 2015). This phloem sap concentration is second only to the New Caledonian tree *Pycnandra acuminata*, which may contain up to 257 g kg^{-1} Ni in the latex (Jaffré *et al.* 1976). The chemical form of Ni was consistently associated with citrate and did not differ between the species in all of the tissues (roots, phloem and leaves) nor in the transport liquids (xylem and phloem) (van der Ent *et al.* 2017a). In *Phyllanthus serpentinus* and *Psychotria gabriellae* from New Caledonia, Ni-malate was reported as the dominant chemical form of Ni within the plant cells (Kersten *et al.* 1980), whereas citrate was found as the major ligand in several other hyperaccumulator plant species, e.g. *P. acuminata*, *Hybanthus caledonicus* (Lee *et al.* 1977, 1978; Kersten *et al.* 1980).

The current research aims to expand the knowledge base on tropical Ni hyperaccumulator plant species by investigating a number of species originating from different families: Rubiaceae (*P. sarmentosa*), Salicaceae (*F. kinabaluensis*) and from different genera from the Phyllanthaceae family (*G. brunneum*, *A. alanbakeri*) using micro-PIXE analysis. Specifically, the tissue-level distribution of Ni and other physiologically relevant elements in these species will be compared with information available for the *Rinorea* spp. and *Phyllanthus* spp. studied previously. Through this analysis we aimed to establish whether patterns of tissue-level elemental distribution are different in phylogenetically distant hyperaccumulator species, and hence whether basic underlying mechanisms of Ni hyperaccumulation may be distinct or similar.

Materials and Methods

Collection and bulk analysis of plant tissue samples

Young plants of *F. kinabaluensis*, *A. alanbakeri*, *G. brunneum* and *P. sarmentosa* were collected in their natural habitats in and near Kinabalu Park in Sabah (Malaysia) on the island of Borneo. These wild-collected plant specimens were subsequently potted in the nursery of the 'Hyperaccumulator Botanical Garden' at Monggis substation of Kinabalu Park and cultivated there for ~1 year. Individuals of *G. brunneum* were growing naturally near the nursery.

Tissue samples including roots, old stems, young stems and leaves of *F. kinabaluensis*, *A. alanbakeri*, *P. sarmentosa* and young stems and leaves of *G. brunneum* grown in cultivation at the Hyperaccumulator Botanical Garden were harvested. Branches, fruits and berries of *P. sarmentosa* and phloem of *A. alanbakeri* were also harvested. Root tissues were thoroughly washed with water to remove potentially particulate (soil) contamination. The plant tissue samples were cut out with a surgical stainless-steel knife directly from the living plants. The samples collected for micro-PIXE analysis were immediately flash-frozen in the field using a cold mirror technique in which the samples were pressed between a large block of copper metal cooled by liquid nitrogen (–196 °C) and a second block of copper attached to a Teflon holder. This ensured extremely fast freezing of the plant tissue samples to prevent cellular damage by ice crystal formation. The samples were then wrapped in aluminium foil and transported in a cryogenic container directly to iThemba LABS in South Africa for analysis. Phloem samples were collected by stripping sections of this tissue from beneath the bark.

Plant tissue subsamples were dried at 70 °C for 5 days in a dehydrating oven for bulk elemental analysis. The dried plant tissue samples were subsequently ground, and a 300-mg fraction was digested using 5 mL concentrated nitric acid (70 %) in a digestion microwave oven (Milestone Start D) for a 45-min programme, and after cooling diluted to 30 mL with ultrapure water. The samples were then analysed by ICP-AES (Varian Vista Pro II) for Na, Mg, Al, P, S, K, Ca, Cr, Mn, Fe, Co, Ni, Cu, and Zn.

Nuclear microprobe elemental analysis of plant tissues

Specimens were removed from the LN_2 storage container and freeze-dried in a Leica EM CFD Cryosorption Freeze Dryer (Leica Microsystems AG, Austria). The freeze-drying process followed a long, 208-h programmed cycle to prevent shrinkage of the tissues. Freeze-dried plant tissues were then hand-cut with a steel razor blade and mounted on specimen holders covered with 0.5 % Formvar film and lightly coated with carbon to prevent charging. Elemental microanalyses were performed using the nuclear microprobe at the Materials Research Department, iThemba LABS, South Africa. The facility and methodology of measurements of biological materials have been reported elsewhere in detail (Prozesky *et al.* 1995; Przybyłowicz *et al.* 1999, 2005).

Nuclear microprobe elemental analysis uses a proton beam of 3 MeV energy, provided by a 6-MV single-ended Van de Graaff accelerator. The proton beam was focussed to a 3 × 3 μm^2 spot and raster-scanned over the areas of interest, using square or rectangular scan patterns with a variable number of pixels (up to 128 × 128). Proton current was restricted to 100–150 pA to minimize specimen beam damage. Proton-induced X-ray emission and proton BS were used simultaneously. Proton-induced X-ray emission spectra were registered with a Si(Li) detector manufactured by PGT (30 mm^2 active area and 8.5 µm Be window) with an additional 125 µm Be layer as an external absorber. The effective energy resolution of the PIXE system (for the Mn Kα line) was 160 eV, measured for individual spectra. The detector was positioned at a take-off angle of 135° and a working distance of 24 mm. The X-ray energy range was set between 1 and 40 keV. Backscattering spectrometry spectra were recorded with an annular Si surface barrier detector (100 µm thick) positioned at an average angle of 176°. Data were acquired in the event-by-event mode. The normalization of results was performed using the integrated beam charge, collected simultaneously from a Faraday cup located behind the specimen and from the insulated specimen holder. The total accumulated charge per scan varied from 0.51 to 3.82 µC.

The concentration and distribution of Si, P, S, Cl, K, Ca, Mn, Fe, Co, Ni, Cu, Zn, Br, Rb and Sr were quantified in the freeze-dried plant tissues of *F. kinabaluensis*, *A. alanbakeri*, *G. brunneum* and *P. sarmentosa*. These quantitative results were obtained by a standardless method using GeoPIXE II software package (Ryan *et al.* 1990a, b; Ryan 2000). The error estimates are extracted from the error matrix generated in the fit, and the minimum detection limits are calculated using the Currie equation (Currie 1968). The detailed calibration of detector efficiency, the thicknesses of selectable X-ray-attenuating filters and studies on the accuracy and precision have been reported elsewhere (van Achterbergh *et al.* 1995). The procedure reported there was used for the PGT Si(Li) detector used in the present study. The calibration of the analytical system was tested by measurements of standards (pure elements and synthetic glasses with known quantities of selected minor elements), the X-ray peaks of which cover practically the whole measurable energy range. Quantitative elemental mapping was performed using Dynamic Analysis method (Ryan and Jamieson 1993; Ryan *et al.* 1995; Ryan 2000). This method generates elemental images, which are (i) overlap-resolved, (ii) with subtracted background and (iii) quantitative, i.e. accumulated in µg g^{-1} dry weight units. Maps were complemented by data extracted from arbitrarily selected micro-areas within scanned plant tissue. Particle-induced X-ray emission and BS spectra were employed to obtain average concentrations from these micro-areas using a

full non-linear deconvolution procedure to fit PIXE spectra (Ryan *et al.* 1990a, b), with matrix corrections based on thickness and matrix composition obtained from the corresponding BS spectra, fitted with a RUMP simulation package (Doolittle 1986) with non-Rutherford cross-sections for C, O, N.

Electron microscopy of freeze-dried plant tissues

Freeze-dried leaf samples (24 h at –80 °C) were sputter-coated with carbon (25 nm) and mounted on stubs. The samples were then imaged with scanning electron microscopy (SEM) on a JEOL JSM-6610.

Results

Bulk chemistry of the studied hyperaccumulator plants

The results of the ICP-AES in plant tissues of *A. alanbakeri*, *G. brunneum*, *P. sarmentosa* and *F. kinabaluensis* are shown in Tables 1 and 2. The mean foliar Ni concentration in *A. alanbakeri* was 4500 μg g^{-1} (range from 280 to 14 700 μg g^{-1}), 20 500 μg g^{-1} in *P. sarmentosa* (range from 9500 to 29 600 μg g^{-1}), 770 μg g^{-1} in *F. kinabaluensis* and 3900 μg g^{-1} in *G. brunneum* (range from 2180 to 5540 μg g^{-1}) (Table 1). In the roots Ni concentration was 970 μg g^{-1} in *A. alanbakeri* and 1090 μg g^{-1} in *P. sarmentosa*. In the old stems its concentration was between 3100 and 8430 μg g^{-1} in *P. sarmentosa* (mean value 6050 μg g^{-1}), while in the young stems the ranges of concentrations were from 580 to 1700 μg g^{-1} in *A. alanbakeri* (mean value 1030 μg g^{-1}) and from 6200 to 8800 μg g^{-1} in *P. sarmentosa* (mean value 7400 μg g^{-1}). The mean foliar concentration of K was 17 100 μg g^{-1} in *A. alanbakeri* (range from 8800 to 22 400 μg g^{-1}), 2880 μg g^{-1} in *P. sarmentosa* (range from 1260 to 4620 μg g^{-1}), 14 000 μg g^{-1} in *F. kinabaluensis* and 5060 μg g^{-1} in *G. brunneum* (range from 4130 to 6280 μg g^{-1}) (Table 2). *Actephila alanbakeri*, *P. sarmentosa* and *F. kinabaluensis* had foliar Ca concentrations ranging between 1520 and 11 300 μg g^{-1} (mean value 5720 μg g^{-1}), between 2600 and 13 500 μg g^{-1} (mean value 6900 μg g^{-1}) and 10 500 μg g^{-1}, respectively, and between 4170 and 5300 μg g^{-1} in *G. brunneum* (mean value 4720 μg g^{-1}). Foliar Mn concentration in *A. alanbakeri* ranged between 50 and 530 (mean value 180 μg g^{-1}), whereas in *P. sarmentosa* it was between 680 and 1550 μg g^{-1} (mean value 1100 μg g^{-1}), between 80 and 140 μg g^{-1} in *G. brunneum* (mean value 110 μg g^{-1}) and 90 μg g^{-1} in *F. kinabaluensis*. Values for Cr, Fe, Co, Cu and Zn were low in the leaves of all of the studied species (Table 1).

Nuclear microprobe microanalyses of the studied hyperaccumulator plants

The results of the nuclear microprobe analysis in anatomical regions of the roots, old stems, young stems and leaves are shown in Tables 3–6, Figs 2–5 and **Supporting Information—Figs S1–S5**.

Roots. The concentrations of Ni in roots of *A. alanbakeri* ranged between 100 and 370 μg g^{-1}; in *P. sarmentosa* they were between 50 and 100 μg g^{-1}, and between 70 and 190 μg g^{-1} in *F. kinabaluensis* (Table 3), whereas Ni was predominantly concentrated in the phloem of *F. kinabaluensis* and *A. alanbakeri*. It also showed high enrichment in the epidermis of *A. alanbakeri* and *F. kinabaluensis* and in some parts of *P. sarmentosa* (Fig. 2; **see Supporting Information—Figs S1 and S2**).

The concentrations of Cl in the roots of *A. alanbakeri* ranged between 3060 and 6300 μg g^{-1}, between 750 and 4070 μg g^{-1} in *P. sarmentosa* and between 670 and 1780 μg g^{-1} in *F. kinabaluensis* (Table 3) with enrichment in the cortex of *A. alanbakeri* and *F. kinabaluensis*, whereas in *P. sarmentosa* it was concentrated in the cortex and phloem (Fig. 2; **see Supporting Information—Figs S1 and S2**). The concentrations of K in *A. alanbakeri* were between 9460 and 14 800 μg g^{-1}, whereas in *P. sarmentosa* it ranged from 3620 to 4600 μg g^{-1} and between 5600 and 9110 μg g^{-1} in *F. kinabaluensis* (Table 3) with strong enrichment in the cortex and phloem of all three species (Fig. 2; **see Supporting Information—Figs S1 and S2**). It was much more concentrated in the phloem of *A. alanbakeri* in comparison with the two other species **[see Supporting Information—Fig. S2]**. The concentrations of Ca in *A. alanbakeri* ranged from 345 to 890 μg g^{-1}, in *P. sarmentosa* from 900 to 2030 μg g^{-1}, and from 740 to 1300 μg g^{-1} in *F. kinabaluensis* (Table 3) with high enrichment in the cortex and phloem of *A. alanbakeri* and *F. kinabaluensis* and in some parts of the phloem of *P. sarmentosa* (Fig. 2; **see Supporting Information—Figs S1 and S2**).

Manganese concentrations in the roots of *A. alanbakeri* were between 30 and 55 μg g^{-1}, between 10 and 30 μg g^{-1} in *P. sarmentosa* and between 6 and 65 μg g^{-1} in *F. kinabaluensis* (Table 3), with strong enrichment in the epidermis and cortex of *A. alanbakeri* and *F. kinabaluensis*, but low and evenly spread in *P. sarmentosa* (Fig. 2; **see Supporting Information—Figs S1 and S2**). The concentrations of Co in roots of all the three species were low with comparable values; in *A. alanbakeri* they ranged between 6 and 20 μg g^{-1}, did not exceed 15 μg g^{-1} in *P. sarmentosa* and were between 6 and 15 μg g^{-1} in *F. kinabaluensis* (Table 3). Cobalt was enriched in the epidermis, cortex and phloem of *A. alanbakeri* and in the epidermis and cortex of *F. kinabaluensis*, but more evenly spread throughout the sections of *P. sarmentosa* (Fig. 2; **see Supporting Information—Figs S1 and S2**).

Old stems. The concentration of Ni was 700 μg g^{-1} in the old stem of *A. alanbakeri*, 250 μg g^{-1} in *P. sarmentosa* and between 100 and 500 μg g^{-1} in *F. kinabaluensis* (Table 4), with enrichment in the cortex and phloem of *F. kinabaluensis* and *A. alanbakeri* and in the pith and xylem of *P. sarmentosa* (Fig. 3; **see Supporting Information—Fig. S3**).

The concentration of Cl in the old stem of *A. alanbakeri* was 1670 μg g^{-1}, whereas in *P. sarmentosa* it was 30 000 μg g^{-1} and between 520 and 540 μg g^{-1} in *F. kinabaluensis* (Table 4) with enrichment in the cortex of *A. alanbakeri* and *F. kinabaluensis* and in the cortex, phloem and xylem of *P. sarmentosa* (Fig. 3; **see Supporting Information—Fig. S3**). The K concentration in *P. sarmentosa* was 27 400 μg g^{-1}, whereas in *A. alanbakeri* it was 11 100 μg g^{-1} and between 7720 and 8230 μg g^{-1} in *F. kinabaluensis* (Table 4) with the highest enrichment in the cortex and phloem of *F. kinabaluensis* and *A. alanbakeri* (Fig. 3; **see Supporting Information—Fig. S3**). In *P. sarmentosa*, this element was more evenly spread and showed enrichment in the part of xylem (Fig. 3). The concentration of Ca in old stem of *A. alanbakeri* was 1800 μg g^{-1} and 2440 μg g^{-1} in *P. sarmentosa*. In *F. kinabaluensis* its concentration ranged from 2340 to 2960 μg g^{-1} (Table 4), with enrichment in the cortex and phloem of *A. alanbakeri* and some 'dots' of enrichment in the cortex, phloem and xylem of *P. sarmentosa*, whereas in *F. kinabaluensis* it was more concentrated in the phloem (Fig. 3; **see Supporting Information—Fig. S3**).

Manganese concentrations in the old stems of *F. kinabaluensis* were between 15 and 100 μg g^{-1}, 60 μg g^{-1} in *A. alanbakeri* and 20 μg g^{-1} in *P. sarmentosa* (Table 4) with Mn enriched in the cortex of *A. alanbakeri*, and *F. kinabaluensis* while it was much more evenly spread in the cortex, xylem and phloem of *P. sarmentosa* (Fig. 3; **see Supporting Information—Fig. S3**). The concentration of Co in *F. kinabaluensis* was between 4 and 14 μg g^{-1}, whereas in *A. alanbakeri* it was 3 μg g^{-1} and below the limit of detection (<5 μg g^{-1}) in *P. sarmentosa* (Table 4). In *F. kinabaluensis* there was a clear enrichment of this element in the cortex and phloem, while in *A. alanbakeri* there was some

Table 1. Concentrations of beneficial and trace elements in plant tissues in *Actephila alanbakeri*, *Glochidion brunneum*, *Psychotria sarmentosa* and *Flacourtia kinabaluensis* (values as ranges and [means] in μg g^{-1} dry weight) analysed by ICP-AES.

Species	*n*	Na	Al	Cr	Mn	Fe	Co	Ni	Cu	Zn
					Leaves					
Actephila alanbakeri	6	30–910 [305]	15–60 [45]	3.0–30 [20]	50–530 [180]	40–100 [80]	10–55 [30]	280–14 700 [4500]	3.0–25 [15]	20–100 [50]
Psychotria sarmentosa	5	90–2400 [1480]	165–3770 [1200]	30–140 [95]	680–1550 [1100]	30–125 [60]	4.0–15 [10]	9500–29 600 [20 500]	4.0–15 [5]	50–100 [75]
Flacourtia kinabaluensis	1	220	50	60	90	70	85	770	25	50
Glochidion brunneum	3	180–570 [395]	30–60 [40]	5–10 [8]	80–140 [110]	10–65 [30]	20–40 [30]	2180–5540 [3900]	2 [2]	10–30 [20]
					Branches					
Psychotria sarmentosa	1	1050	65	15	40	10	10	4820	5	30
					Fruit					
Psychotria sarmentosa	1	850	430	10	290	25	10	3920	10	20
					Berries					
Psychotria sarmentosa	1	95	70	10	50	10	10	6820	5	40
					Wood					
Actephila alanbakeri	1	200	5	5	40	15	10	270	2	10
					Young stems					
Actephila alanbakeri	3	240–390 [300]	5–110 [10]	1.0–2.0 [2.0]	70–290 [210]	10–30 [20]	5.0–10 [10]	580–1700 [1030]	2.0–3.0 [2.5]	20–70 [40]
Psychotria sarmentosa	3	1060–3150 [1960]	110–190 [140]	30–50 [40]	100–270 [190]	15–30 [20]	6.0–9.0 [7.5]	6200–8800 [7400]	3.0–6.00 [5.00]	20–90 [50]
					Old stems					
Psychotria sarmentosa	3	220–1510 [1050]	30–320 [135]	20–170 [80]	30–220 [150]	15–20 [20]	10–15 [10]	3100–8430 [6050]	3.0–10 [4.50]	20–30 [20]
					Phloem					
Actephila alanbakeri	1	250	30	2	350	50	15	2500	4	120
					Roots					
Actephila alanbakeri	1	40	65	15	30	300	8	970	2	40
Psychotria sarmentosa	1	1500	405	20	70	270	8	1090	5	15

Table 2. Concentrations of macroelements in plant tissues in *Actephila alanbakeri*, *Glochidion brunneum*, *Psychotria sarmentosa* and *Flacourtia kinabaluensis* (values as ranges and [means] in μg g^{-1} dry weight) analysed by ICP-AES.

Species	*n*	Mg	P	S	K	Ca
			Leaves			
Actephila alanbakeri	6	1280–6500 [4100]	300–1440 [852]	610–2770 [1770]	8800–22 400 [17 100]	1520–11 300 [5720]
Psychotria sarmentosa	5	4380–8100 [6000]	130–600 [330]	1360–1900 [1700]	1260–4620 [2880]	2600–13 500 [6900]
Flacourtia kinabaluensis	1	5400	810	2100	14 000	10 500
Glochidion brunneum	3	1320–2710 [2160]	160–210 [190]	530–700 [640]	4130–6280 [5060]	4170–5300 [4720]
			Branches			
Psychotria sarmentosa	1	490	65	370	2430	850
			Fruit			
Psychotria sarmentosa	1	3370	530	1040	5420	3960
			Berries			
Psychotria sarmentosa	1	3720	325	515	7800	2660
			Wood			
Actephila alanbakeri	1	520	270	290	1670	200
			Young stems			
Actephila alanbakeri	3	1590–3460 [2620]	795–1210 [1060]	410–970 [680]	7230–10 600 [8880]	1280–6770 [3410]
Psychotria sarmentosa	3	1000–2090 [1500]	85–410 [210]	840–1260 [1010]	3710–6710 [5000]	1880–5560 [3590]
			Old stems			
Psychotria sarmentosa	3	440–2440 [1150]	40–250 [140]	370–550 [460]	575–6530 [2730]	570–3540 [2000]
			Phloem			
Actephila alanbakeri	1	4260	290	840	12 800	2090
			Roots			
Actephila alanbakeri	1	1260	350	215	3900	310
Psychotria sarmentosa	1	650	110	380	910	1370

enrichment in the epidermis, in comparison with the other tissue parts (Fig. 3; **see Supporting Information—Fig. S3**).

Young stems. The Ni concentration in the young stem of *A. alanbakeri* was 1160 μg g^{-1}, whereas in *G. brunneum* it was 175 μg g^{-1}, 190 μg g^{-1} in *P. sarmentosa* and 100 μg g^{-1} in *F. kinabaluensis* (Table 5). In *A. alanbakeri*, there was a strong Ni enrichment in the phloem and relatively low enrichment in the pith and primary xylem (Fig. 4). In *G. brunneum*, Ni was more evenly spread throughout the whole stem section, with slight enrichment in the pith and xylem (Fig. 4). The enrichment in the pith and xylem was much more pronounced in *P. sarmentosa* (Fig. 4); this pattern was also visible in *F. kinabaluensis* (Fig. 4), but less clear because of overall lower concentration of Ni in the measured section.

The concentration of Cl in young stem of *A. alanbakeri* was 1600 μg g^{-1}, whereas in *G. brunneum* it was 13 300 μg g^{-1}, 6900 μg g^{-1} in *P. sarmentosa* and 700 μg g^{-1} in *F. kinabaluensis* (Table 5) with Cl concentrated in the cortex of *A. alanbakeri*, *P. sarmentosa*, *F. kinabaluensis* and in the cortex, phloem and xylem of *G. brunneum* (Fig. 4). The highest concentration of K in the young stems was in *G. brunneum*, where it reached 21 400 μg g^{-1}, whereas in *A. alanbakeri* it was 11 700 μg g^{-1}, 13 500 μg g^{-1} in *P. sarmentosa* and 13 600 μg g^{-1} in *F. kinabaluensis* (Table 5) with strong enrichment in the cortex, phloem, xylem and pith of *A. alanbakeri*, in the cortex and phloem of *G. brunneum*, *P. sarmentosa* and *F. kinabaluensis*, and some enrichment in the xylem and phloem of *P. sarmentosa* (Fig. 4). There was significant depletion of this element in the pith of *G. brunneum* in comparison with the other species. The concentration of Ca in young stem of *A. alanbakeri* was 2950 μg g^{-1}, 2570 μg g^{-1} in *F. kinabaluensis*, 1540 and 1370 μg g^{-1} in *P. sarmentosa* (Table 5). Many small 'dots' (Ca-oxalate crystals) were visible in the pith and phloem of *P. sarmentosa* and *F. kinabaluensis*. In *P. sarmentosa*, there was an overall enrichment in the epidermis, cortex and phloem, whereas in *A. alanbakeri*, it was more concentrated in the epidermis, phloem and pith (Fig. 4).

The concentrations of Mn were very low in all studied species, at the 15–30 μg g^{-1} level with the exception of *A. alanbakeri*, where the average value for the whole section was 155 μg g^{-1} (Table 5), with enrichment in the epidermis, cortex and phloem (Fig. 4). The concentrations of Co were even lower, below the limits of detection with the exception of *A. alanbakeri* where Co was found at the 3 μg g^{-1} level (Table 5).

Leaves. The concentrations of Ni in the leaves of *G. brunneum* were 1060 μg g^{-1}, the only one species where the hyperaccumulation threshold was exceeded in the leaves' sections; between 270 and 740 μg g^{-1} in *A. alanbakeri*, from 60 to 250 μg g^{-1} and from 85 to 360 μg g^{-1} in *P. sarmentosa* and *F. kinabaluensis*, respectively (Table 6). Nickel was mainly distributed in the lower and upper epidermal cells of the leaves of all the studied species. However, in *A. alanbakeri*, Ni was also

Table 3. Average elemental concentrations (micro-PIXE, μg g^{-1} dry weight) in the sections of the roots of *Actephila alanbakeri*, *Psychotria sarmentosa* and *Flacourtia kinabaluensis* (values as ranges and [mean values]).

n	Si	P	S	Cl	K	Ca	Cr	Mn	Fe	Co	Ni	Cu	Zn
						Actephila alanbakeri							
3	4810–9830 [6060]	330–625 [515]	1890–3060 [2317]	3060–6300 [4863]	9460–14 800 [12 553]	345–890 [585]	30–40 [33]	30–55 [45]	770–1370 [1077]	6–20 [12]	100–370 [253]	3.5–4.5 [4]	40–70 [53]
						Psychotria sarmentosa							
2	1710–9200 [5455]	200–220 [210]	2670–9800 [6235]	750–4070 [2410]	3620–4600 [4110]	900–2030 [1465]	1–40 [20]	10–30 [20]	120–1340 [730]	1–15 [7.5]	50–100 [75]	<2.1	6.5–20 [13.3]
						Flacourtia kinabaluensis							
3	1640–9500 [4900]	160–250 [200]	480–11 700 [4300]	670–1780 [1120]	5600–9110 [7170]	740–1300 [1030]	7–85 [39]	6–65 [37]	250–1580 [820]	6–15 [9]	70–190 [120]	<3.5	10–30 [20]

Table 4. Average elemental concentrations (micro-PIXE, μg g^{-1} dry weight) in the sections of the old stems of *Actephila alanbakeri*, *Psychotria sarmentosa* and *Flacourtia kinabaluensis*. For single measurements errors of analysis (± SD) are shown in brackets. For $n > 1$ the results are shown as ranges and [mean values].

n	Si	P	S	Cl	K	Ca	Cr	Mn	Fe	Co	Ni	Cu	**Zn**
						Actephila alanbakeri							
1	4070 (425)	380 (30)	620 (30)	1670 (20)	11 100 (50)	1800 (30)	15 (1.0)	60 (2)	500 (10)	3 (3)	700 (20)	3.5 (1.0)	90 (3)
						Psychotria sarmentosa							
1	870 (250)	1050 (80)	1310 (54)	30 000 (270)	27 400 (170)	2440 (70)	30 (1)	20 (5)	80 (7)	<5	250 (20)	5 (2)	10 (1)
						Flacourtia kinabaluensis							
2	5100–13 100 [9100]	310–417 [364]	440–1970 [1205]	520–540 [530]	7720–8230 [7975]	2340–2960 [2650]	5.5–40 [23]	15–100 [58]	410–1520 [965]	4–14 [9]	100–500 [300]	<3	20–35 [28]

Table 5. Average elemental concentrations (micro-PIXE, μg g^{-1} dry weight) in the sections of the young stems of *Actephila alanbakeri*, *Glochidion brunneum*, *Psychotria sarmentosa* and *Flacourtia kinabaluensis*. Errors of analysis (+ SD) are shown in brackets.

Si	P	S	Cl	K	Ca	Cr	Mn	Fe	Co	Ni	Cu	Zn
					Actephila alanbakeri							
4420 (390)	1620 (130)	2000 (110)	1600 (40)	11 700 (80)	2950 (30)	14.5 (1)	155 (6)	770 (15)	3 (3)	1160 (30)	5 (1)	230 (6)
					Glochidion brunneum							
140 (140)	350 (55)	1740 (40)	13 300 (80)	21 400 (90)	1540 (50)	<1.5	30 (4)	4 (3)	<7	175 (10)	4.5 (0.5)	9.0 (0.5)
					Psychotria sarmentosa							
1100 (115)	510 (40)	1850 (25)	6900 (30)	13 500 (80)	1370 (30)	95 (3)	15 (5)	65 (5)	<3	190 (10)	2.0 (0.5)	10 (1)
					Flacourtia kinabaluensis							
1010 (100)	640 (35)	2020 (80)	700 (40)	13 600 (80)	2570 (50)	<2.2	15 (1.0)	90 (5)	<5	100 (10)	<3.5	30 (2)

Table 6. Average elemental concentrations (micro-PIXE, μg g^{-1} dry weight) in the sections of the leaves of *Actephila alanbakeri*, *Glochidion brunneum*, *Psychotria sarmentosa* and *Flacourtia kinabaluensis*. For single measurements errors of analysis (+ SD) are shown in brackets. For $n > 1$ the results are shown as ranges and [mean values].

n	Si	P	S	Cl	K	Ca	Cr	Mn	Fe	Co	Ni	Cu	Zn
						Actephila alanbakeri							
2	190–480 [2135]	220–1000 [610]	580–1090 [835]	4200–4620 [4410]	12 800–15 800 [14 300]	700–6800 [3750]	0.4–11 [5]	90–390 [240]	20–590 [305]	0.2–7 [4]	270–740 [505]	<5	15–61 [38]
						Glochidion brunneum							
1	2420 (300)	<85	1170 (40)	17 300 (100)	38 200 (170)	3340 (100)	<3	110 (10)	25 (10)	<20	1060 (60)	<5	20 (2)
						Psychotria sarmentosa							
3	740–1850 [1330]	300–670 [490]	1250–2500 [2070]	12 400–16 400 [14 030]	2300–7800 [4560]	690–1970 [1200]	1.1–40 [20]	25–120 [70]	80–200 [140]	<2	60–250 [170]	<3.5	5.5–45 [22]
						Flacourtia kinabaluensis							
3	410–2780 [1720]	250–280 [263]	400–1250 [690]	1100–4300 [2300]	2650–10 300 [5330]	900–3470 [1770]	0.4–6 [2]	4–15 [10]	180–250 [210]	2–15 [7]	85–360 [195]	<5	8–45 [21]

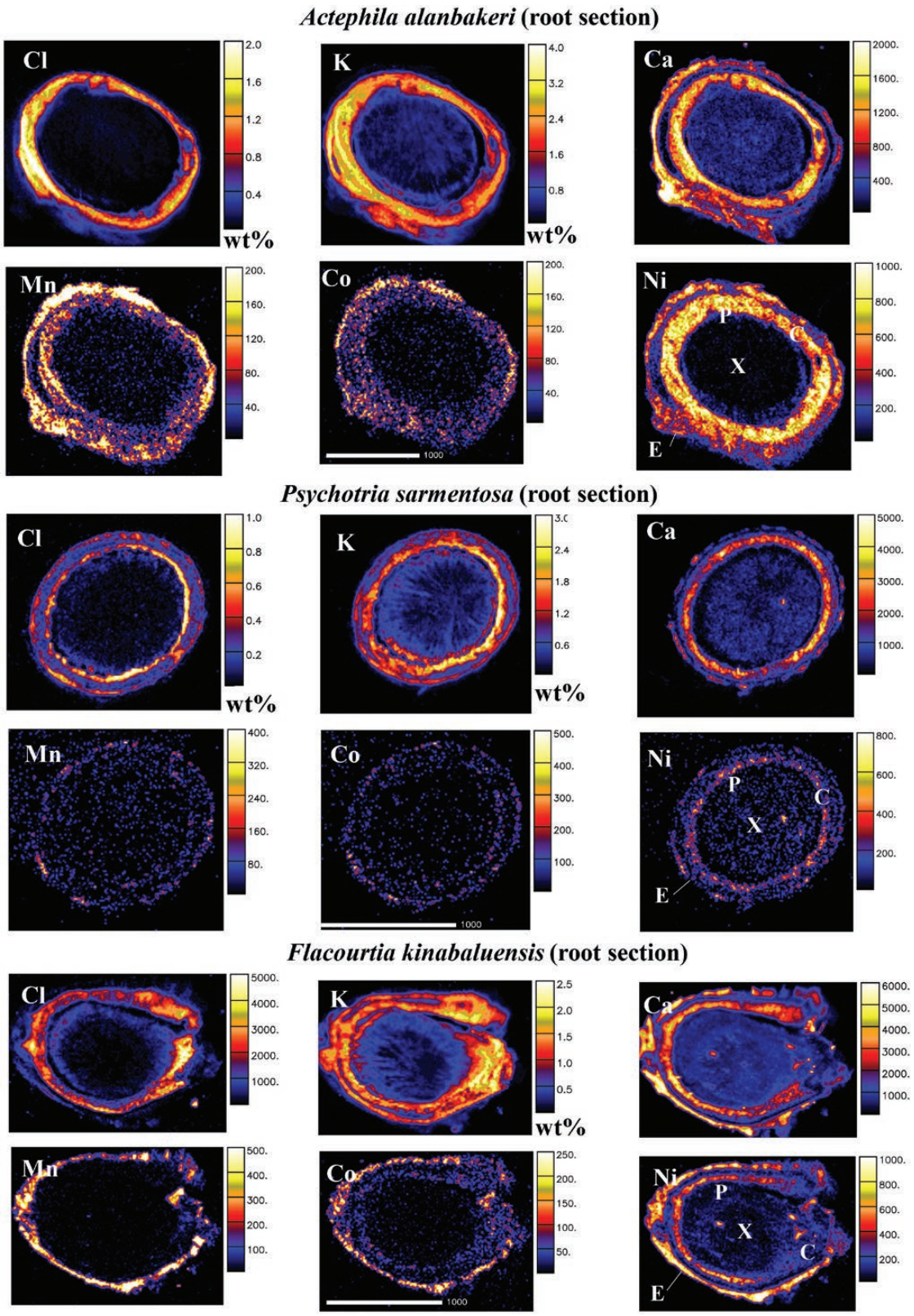

Figure 2. Micro-PIXE quantitative elemental maps of root cross-sections of *Actephila alanbakeri*, *Psychotria sarmentosa* and *Flacourtia kinabaluensis*. Concentration scale in wt% dry weight or in μg g^{-1} dry weight. Abbreviations of anatomical features: C, cortex; E, epidermis; P, phloem; and X, xylem.

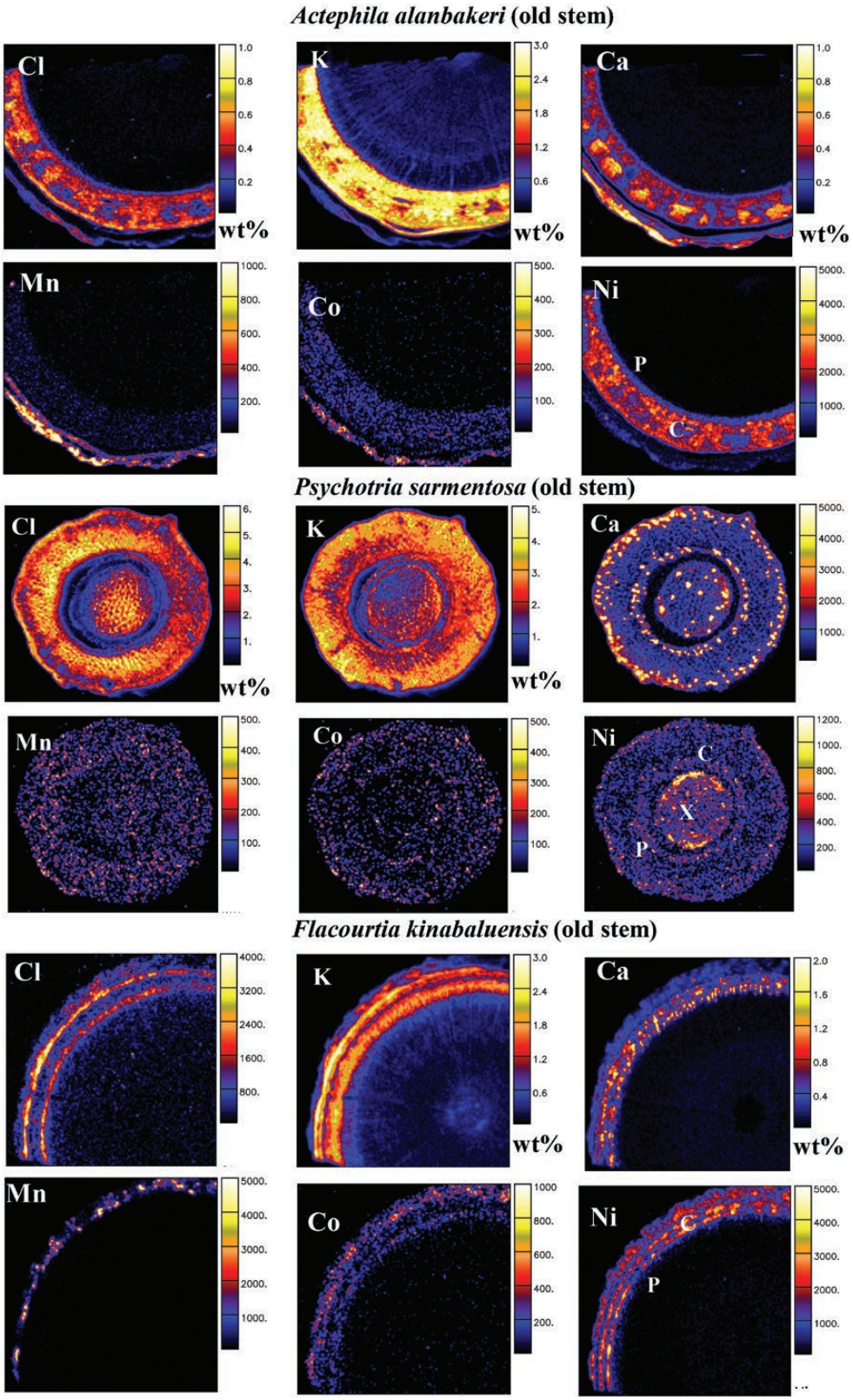

Figure 3. Micro-PIXE quantitative elemental maps of old stem cross-sections of *Actephila alanbakeri*, *Psychotria sarmentosa* and *Flacourtia kinabaluensis*. Concentration scale in wt% dry weight or in μg g^{-1} dry weight. Abbreviations of anatomical features: C, cortex; P, phloem; and X, xylem.

strongly enriched in the spongy and palisade mesophyll (Fig. 5; **see Supporting Information—Fig. S5**). Nickel concentration was lower in the phloem and xylem of all of the species (Fig. 5; **see Supporting Information—Figs S4 and S5**).

The concentration of Cl in *A. alanbakeri* ranged between 4200 and 4620 μg g^{-1}, 17 300 μg g^{-1} in *G. brunneum*, between 12 400 and 16 400 μg g^{-1} in *P. sarmentosa* and from 1100 to 4300 μg g^{-1} in *F. kinabaluensis* (Table 6) with enrichment in the xylem of

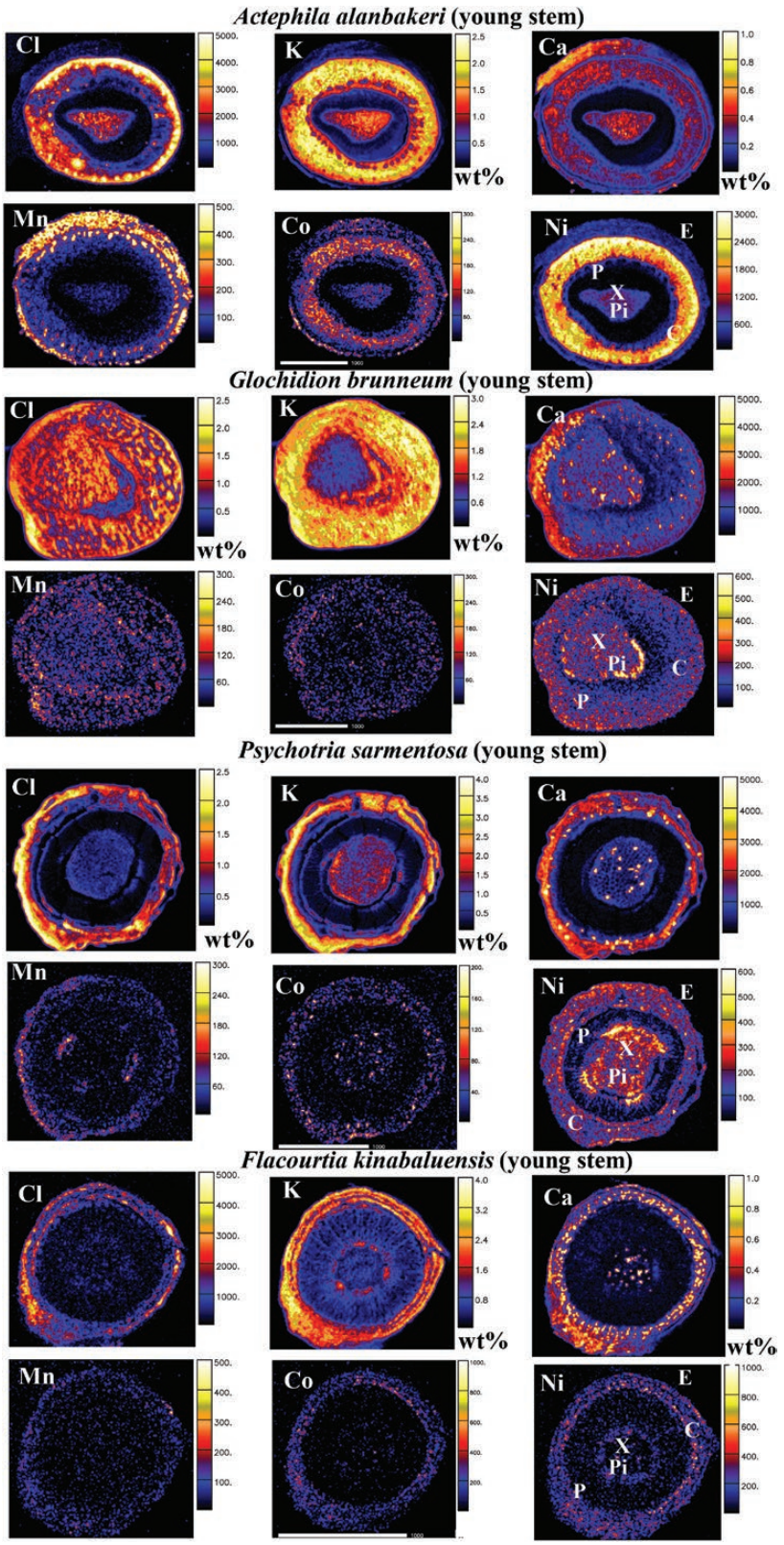

Figure 4. Micro-PIXE quantitative elemental maps of young stem cross-sections of *Actephila alanbakeri*, *Glochidion brunneum*, *Psychotria sarmentosa* and *Flacourtia kinabaluensis*. Concentration scale in wt% dry weight or in μg g^{-1} dry weight. Abbreviations of anatomical features: C, cortex; E, epidermis; Pi, pith; P, phloem; and X, xylem.

A. alanbakeri, spongy mesophyll of *G. brunneum*, upper and lower epidermis and palisade mesophyll of *P. sarmentosa* and xylem and phloem of *F. kinabaluensis* (Fig. 5; **see Supporting Information—Figs S4 and S5**). Potassium concentrations in the leaves of *G. brunneum* were 38 200 μg g^{-1}, between 12 800 and 15 800 μg g^{-1} in *A. alanbakeri*, between 2650 and 10 300 μg g^{-1} in *F. kinabaluensis* and from 2300 to 7800 μg g^{-1} in *P. sarmentosa*. In all of the studied species, K was strongly enriched in the spongy

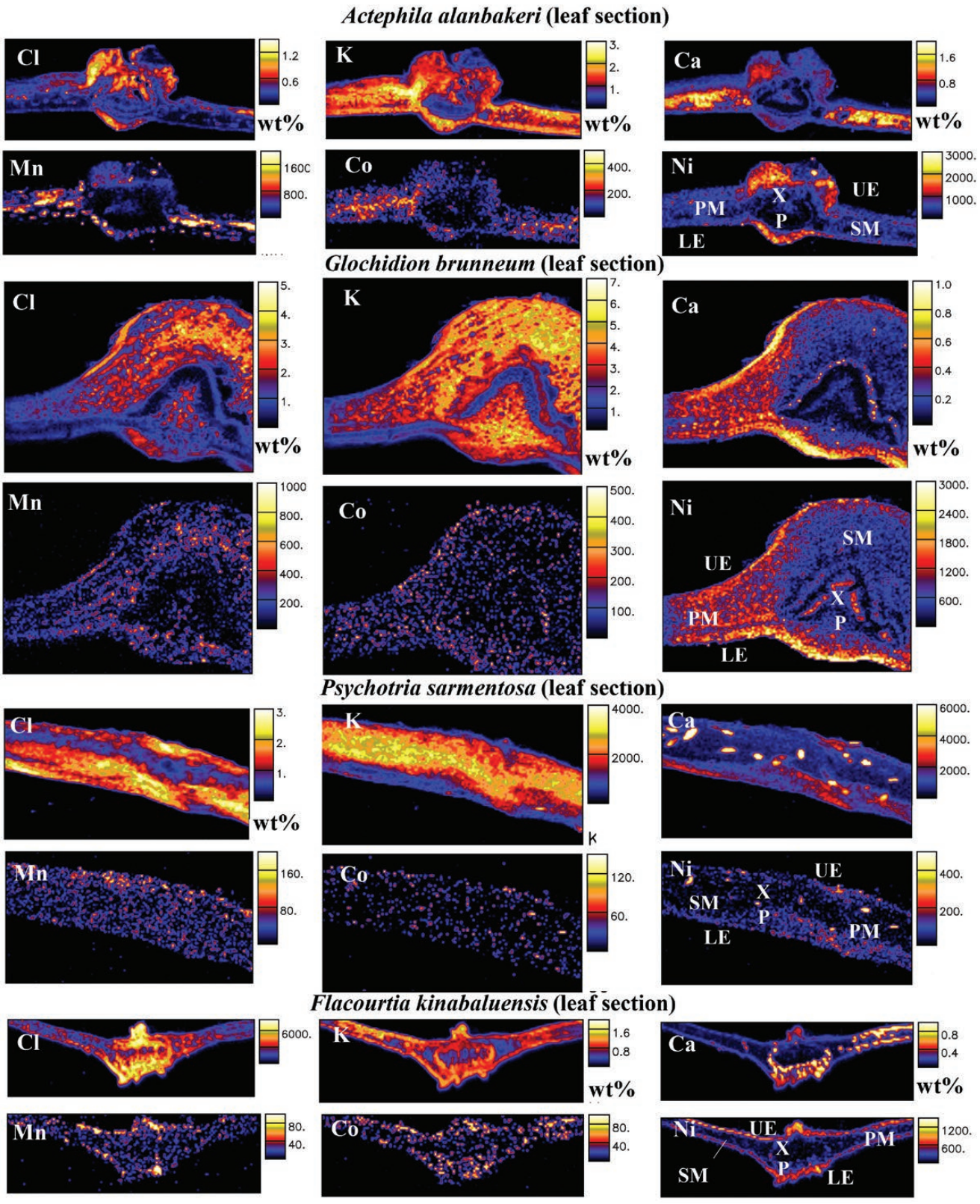

Figure 5. Micro-PIXE quantitative elemental maps of leaf cross-sections of *Actephila alanbakeri*, *Glochidion brunneum*, *Psychotria sarmentosa* and *Flacourtia kinabaluensis*. Concentration scale in wt% dry weight or μg g^{-1} dry weight. Abbreviations of anatomical features: UE, upper epidermis; LE, lower epidermis; PM, palisade mesophyll; SM, spongy mesophyll; P, phloem; and X, xylem.

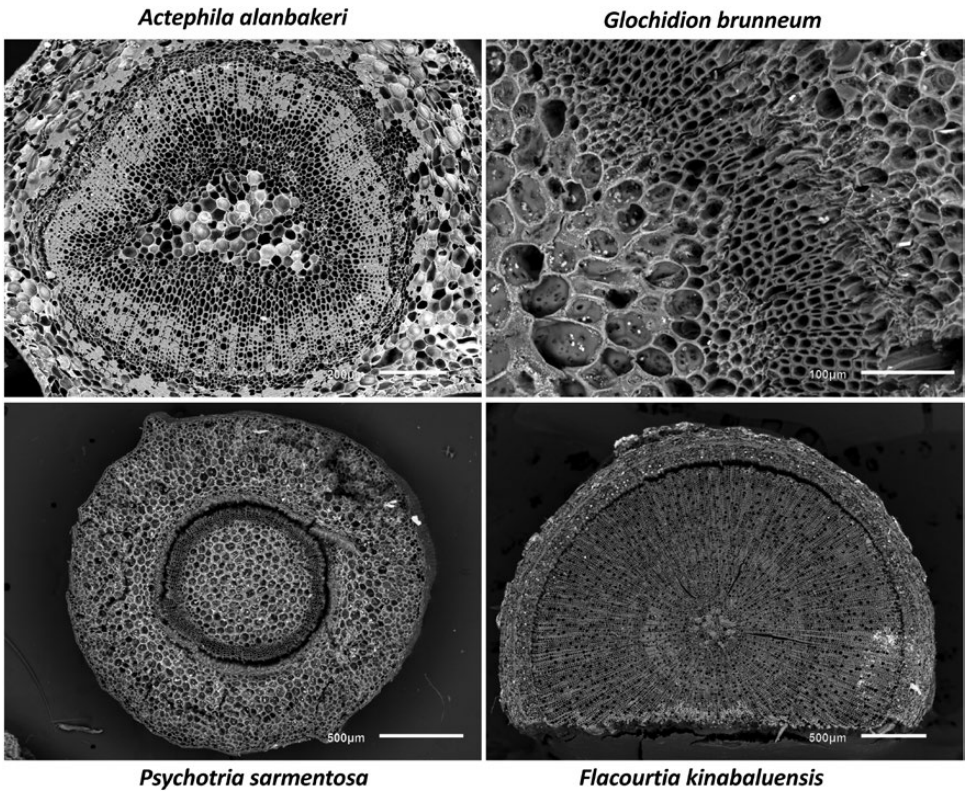

Figure 6. Scanning electron microscopy images of freeze-dried petiole cross-sections of *Actephila alanbakeri*, *Psychotria sarmentosa*, *Glochidion brunneum* and *Flacourtia kinabaluensis*.

and palisade mesophyll. There was also enrichment of K in the phloem of *F. kinabaluensis* and *G. brunneum* and in the xylem of *P. sarmentosa* (Fig. 5; **see Supporting Information—Figs S4 and S5**). Calcium in *A. alanbakeri* was between 700 and 6800 µg g^{-1}, 3340 µg g^{-1} in the leaves of *G. brunneum*, between 900 and 3470 µg g^{-1} in *F. kinabaluensis* and between 690 and 1970 µg g^{-1} in the leaves of *P. sarmentosa* (Table 6) with enrichment in the spongy and palisade mesophyll of *A. alanbakeri* and *G. brunneum* and also in the upper and lower epidermis of *G. brunneum*, and in palisade mesophyll and phloem of *F. kinabaluensis* (Fig. 5; **see Supporting Information—Figs S4 and S5**). Small 'dots' highly enriched in Ca were also visible in the spongy and palisade mesophyll of *P. sarmentosa* (Fig. 5; **see Supporting Information—Fig. S4**).

The concentrations of Mn in *A. alanbakeri* were between 90 and 390 µg g^{-1}, whereas in *G. brunneum* it was 110 µg g^{-1} and ranged from 25 to 120 µg g^{-1} in *P. sarmentosa* and between 4 and 15 µg g^{-1} in *F. kinabaluensis* (Table 6) with some enrichment in the spongy and palisade mesophyll of *A. alanbakeri* and in the upper epidermis of *F. kinabaluensis* (Fig. 5). Cobalt concentrations in the leaves of all the studied species were low (Table 6) with some 'dots' of Co enrichment visible in the epidermis and spongy mesophyll of *A. alanbakeri* and *F. kinabaluensis* (Fig. 5; **see Supporting Information—Figs S4 and S5**).

Scanning electron microscopy

The SEM images show that the freeze-dried petioles of *A. alanbakeri*, *P. sarmentosa*, *F. kinabaluensis* and *G. brunneum* have thick cuticle, multiseriate epidermis, and closely intact xylem and phloem (Fig. 6). This visually confirms that the very slow and low-temperature lyophilization process has left the (sub) cellular structures intact for the micro-PIXE analysis, and that elemental redistribution or other sample degradation is highly unlikely.

Discussion

The plant tissue elemental concentrations reported in this study originate from samples collected from wild populations of *P. sarmentosa*, *G. brunneum*, *A. alanbakeri*, and *F. kinabaluensis* growing on ultramafic soil at Kinabalu Park. In comparison, the plant tissue samples used for the nuclear microprobe investigations originated from plants grown on ultramafic soil in a horticultural setting (Hyperaccumulator Botanical Garden) at Kinabalu Park. The ultramafic potting soil (Mollic Leptosol Hypermagnesic) contains far lower concentrations of plant-available Ni than the ultramafic soil (Hypermagnesic Cambisol) from the native populations (van der Ent *et al.* 2017b). In combination with the small pot size (2- to 3-L), this resulted in relatively low (<3000 µg g^{-1}) foliar Ni concentrations compared to wild material (>10 000 µg g^{-1}). This finding was unexpected, but has since been observed in a dedicated experiment on the effect of pot size on Ni hyperaccumulation in the temperate herb *Alyssum corsicum* (Chaney *et al.* 2017). Elements other than Ni may have also been affected, but conceivably only P and K, which are plant-essential macronutrients that are typically present in limited amounts in the ultramafic soils of Sabah (van der Ent *et al.* 2016).

The results from this study showed that the highest Ni concentrations are in the foliar epidermal cells of all four species. Similarly, in *Rinorea* cf. *bengalensis* and *P. rufuschaneyi*, Ni is also enriched in the foliar epidermal cells (van der Ent *et al.* 2017a). Boyd and Martens (1992) postulated that Ni enrichment

in epidermal cells deters herbivory. However, Mesjasz-Przybyłowicz *et al.* (2016a) argued that this hypothesis would only make sense if symmetrical accumulation of Ni took place in both the upper and lower epidermis, as insect herbivores feed on both sides. Localization of Ni in epidermal cells has further been hypothesized to aid in osmoregulation and drought tolerance by increasing the water potential in the leaves (Severne 1974; Baker and Walker 1990; Boyd and Martens 1992; Mesjasz-Przybyłowicz *et al.* 1996). Preferential localization of Ni in the upper epidermal cell has also been suggested by Robinson *et al.* (2003) to act as a protection for the underlying chlorophyll against ultraviolet radiation. Nickel enrichment in the epidermal parts of leaves is a typical distribution pattern encountered in the majority of studied Ni hyperaccumulator plants to date from diverse phylogenetic and geographical affinities, e.g. *Senecio coronatus*, *S. anomalochrous* and *Berkheya zeyheri* subsp. *rehmannii* var. *rogersiana* (Mesjasz-Przybyłowicz *et al.* 1994, 1996, 2001) from South Africa; *Hybanthus floribundus* subsp. *floribundus* (Kachenko *et al.* 2008) and *Stackhousia tryonii* (Bhatia *et al.* 2004) from Australia; *Alyssum murale* (Broadhurst *et al.* 2004a; McNear *et al.* 2005), *A. bertolonii*, *A. lesbiacum* and *Noccaea goesingense* (Küpper *et al.* 2001) from Europe. An exception to this rule is *Berkheya coddii* (Asteraceae) where Ni is strongly enriched in the leaf veins and mesophyll, whilst the concentrations in the epidermis are relatively lower (Budka *et al.* 2005; Mesjasz-Przybyłowicz and Przybyłowicz 2011, 2020).

Different species of the Ni hyperaccumulator, *Alyssum*, have been reported to have Ni concentrated along with other elements in certain plant tissues. Accumulation of Ni, Mn and Ca was reported by Broadhurst *et al.* (2004b) at the base of *Alyssum* leaf trichomes. Subsequent studies by Broadhurst *et al.* (2009) also revealed a concentration of Ni and Mn only in trichome bases and in cells adjacent to the trichomes of *A. murale* and *A. corsicum*. In this study, the epidermal distribution of Ni as observed in the studied species is similar to that of the distribution of Ca and Cl in *P. sarmentosa* and *G. brunneum*, respectively. Simultaneous accumulation of other potentially toxic trace elements in plant tissues other than Ni such as Mn, Zn and Co has further been suggested by Boyd (2012) to deter herbivory.

Moreover, this study also revealed similar distribution patterns of K in the spongy and palisade mesophyll of the studied species. Calcium was also found enriched in the spongy and palisade mesophyll of *G. brunneum*, whereas in *A. alanbakeri*, both Ca and Ni were strongly enriched in the spongy and palisade mesophyll. This pattern of distribution may be explained by the essential requirement for K, Ca and Ni as plant nutrients by the studied species. Some Mn enrichment in the spongy and palisade mesophyll of *A. alanbakeri* and in the upper epidermis of *F. kinabaluensis* was also found in this study. On the other hand, Mn was found sequestered in the palisade mesophyll cells of the Mn hyperaccumulators *Gossia bidwillii*, *Virotia neurophylla*, *Macadamia integrifolia* and *M. tetraphylla* (Fernando *et al.* 2006a, b) where the authors indicated this to be due to the species high demand for Mn as part of the active centre of the oxygen-evolving complex. In *G. fragrantissima*, Co and Zn were found primarily localized in foliar epidermal cells whilst Mn and Ni were concentrated in the palisade layer (Fernando *et al.* 2013). Previous studies by Brooks *et al.* (1981) and Bidwell *et al.* (2002) have revealed that the Mn hyperaccumulators *Alyxia* sp. and *G. bidwillii* accumulate Mn at the expense of K and Mg. Cobalt distribution in *A. murale* was concentrated in the apoplast, which forms a Co-rich mineral precipitates on the foliar surface (Tappero *et al.* 2007). In comparison for *Glochidion* cf. *sericeum*, Co exudate was reported on the leaf surface in the form of lesions (van der Ent *et al.* 2018), where it was argued by the later authors to be due to the exposure of aerial oxygen that consequently led to oxidation of Co^{2+} to Co^{3+} on their leaf surfaces. However, in this study, minor Co was observed in the epidermis and spongy mesophyll of *A. alanbakeri* and *F. kinabaluensis*.

The phloem bundles are important tissues of Ni accumulation for the woody hyperaccumulators, such as *P. balgooyi*, *P. rufuschaneyi* and *Rinorea* cf. *bengalensis*, with up to 169 g kg^{-1} Ni in the phloem sap in *P. balgooyi* (Mesjasz-Przybyłowicz *et al.* 2016a; van der Ent *et al.* 2017a). High concentrations of Ni in the phloem have also been reported in herbaceous plants such as *S. coronatus* (Mesjasz-Przybyłowicz *et al.* 1997, 2007), *A. murale* (McNear *et al.* 2005; Tappero *et al.* 2007), *B. coddii* (Orłowska *et al.* 2013) and *B. zeyheri* subsp. *rehmannii* var. *rogersiana* (Mesjasz-Przybyłowicz *et al.* 2016b). This aligns with the results of this study on *F. kinabaluensis*, *P. sarmentosa* and *A. alanbakeri* with Ni enrichment in the phloem. In comparison with the New Caledonian Ni hyperaccumulator plants including *Homalium francii* (Phyllanthaceae), *Hybanthus austrocaledonicus* (Rubiaceae) and *P. gabriellae* (Salicaceae), Ni is also strongly localized in the epidermal cells and phloem bundles (Gei *et al.* 2020; Paul *et al.* 2020), and likewise in *Geissois pruinosa* (Cunoniaceae). However, *P. acuminata* (Sapotaceae) has Ni-rich laticifers, which constitute an independent network of cells parallel to the vascular bundles (Gei *et al.* 2020). In addition to the elevated concentrations of K, Ca, Cl, Mn and Co in the phloem of the studied species, these elements have also been found in the present study to be enriched in the cortex and epidermis of young stems, old stems and roots.

Even though Ni hyperaccumulation has ostensibly evolved numerous times independently in distant phylogenetic lineages in different areas around the world, the physiological mechanisms, as inferred from elemental localization, are convergent in these tropical woody species from Borneo Island.

Supporting Information

The following additional information is available in the online version of this article—

Figure S1. Micro-PIXE elemental maps of *Flacourtia kinabaluensis* root section. Concentration scale in wt% dry weight or μg g^{-1} dry weight.

Figure S2. Micro-PIXE elemental maps of *Actephila alanbakeri* root section. Concentration scale in wt% dry weight or μg g^{-1} dry weight.

Figure S3. Micro-PIXE elemental maps of *Flacourtia kinabaluensis* old stem section.

Figure S4. Micro-PIXE elemental maps of *Psychotria sarmentosa* leaf section.

Figure S5. Micro-PIXE elemental maps of *Actephila alanbakeri* leaf section.

Sources of Funding

This research was undertaken at the nuclear microprobe facility of iThemba Laboratory for Accelerator Based Sciences in South Africa. F.A. is the recipient of a UQ Graduate School Scholarship (UQGSS) from The University of Queensland. W.J.P. and J.M.-P. are recipients of the South African National Research Foundation incentive grants no. 114693 and 114694, respectively.

Conflict of Interest

None declared.

Contributions by the Authors

A.V.D.E and J.M.P. planned and designed the research. J.M.P. collected the specimens and performed cryopreparation in the field. J.M.P. and W.P. conducted the micro-PIXE experiments and analysed the PIXE data. All authors wrote the manuscript.

Acknowledgements

We acknowledge Sabah Parks for permission to conduct research in Kinabalu Park, and the Sabah Biodiversity Council for research permits. We thank Rimi Repin, Rositti Karim, Sukaibin Sumail (Sabah Parks) and Postar Miun (Sabah Forestry Department) for their help and expertise in the field. The authors acknowledge the facilities, and the scientific and technical assistance, of the Australian Microscopy & Microanalysis Research Facility at the Centre for Microscopy and Microanalysis, The University of Queensland.

Literature Cited

Baker AJM, Brooks RR. 1988. Botanical exploration for minerals in the humid tropics. *Journal of Biogeography* **15**:221–229.

Baker AJM, Walker PL. 1990. Ecophysiology of metal uptake by tolerant plants. In: Shaw AJ, ed. *Heavy metal tolerance in plants: evolutionary aspects*. Boca Raton, FL: CRC Press Inc., 155–157.

Bani A, Echevarria G, Zhang X, Benizri E, Laubie B, Morel JL, Simonnot MO. 2015. The effect of plant density in nickel-phytomining field experiments with *Alyssum murale* in Albania. *Australian Journal of Botany* **63**:72–77.

Beaman JH. 2005. Mount Kinabalu: hotspot of plant diversity in Borneo. *Biologiske Skrifter* **55**:103–127.

Bhatia NP, Walsh KB, Orlic I, Siegele R, Ashwath N, Baker AJM. 2004. Studies on spatial distribution of nickel in leaves and stems of the metal hyperaccumulator *Stackhousia tryonii* Bailey using nuclear microprobe (micro-PIXE) and EDXS techniques. *Functional Plant Biology* **31**:1061–1074.

Bidwell SD, Woodrow IE, Batianoff GN, Sommer-Knudsen J. 2002. Hyperaccumulation of manganese in the rainforest tree *Austromyrtus bidwillii* (Myrtaceae) from Queensland, Australia. *Functional Plant Biology* **29**:899–905.

Boyd RS. 2012. Plant defense using toxic inorganic ions: conceptual models of the defensive enhancement and joint effects hypotheses. *Plant Science* **195**:88–95.

Boyd RS, Martens SN. 1992. The raison d'etre for metal hyperaccumulation by plants. In: Baker AJM, Proctor J, Reeves RD, eds. *The vegetation of ultramafic (serpentine) soils*. Andover, UK: Intercept Ltd, 279.

Broadhurst CL, Chaney RL, Angle JS, Erbe EF, Maugel TK. 2004a. Nickel localization and response to increasing Ni soil levels in leaves of the Ni hyperaccumulator *Alyssum murale*. *Plant and Soil* **265**:225–242.

Broadhurst CL, Chaney RL, Angle JS, Maugel TK, Erbe EF, Murphy CA. 2004b. Simultaneous hyperaccumulation of nickel, manganese, and calcium in *Alyssum* leaf trichomes. *Environmental Science & Technology* **38**:5797–5802.

Broadhurst CL, Tappero RV, Maugel TK, Erbe EF, Sparks DL, Chaney RL. 2009. Interaction of nickel and manganese in accumulation and localization in leaves of the Ni hyperaccumulators *Alyssum murale* and *Alyssum corsicum*. *Plant and Soil* **314**:35–48.

Brooks RR, Robinson BH. 1998. The potential use of hyperaccumulators and other plants for phytomining. In: Brooks RR, ed. *Plants that hyperaccumulate heavy metals. Their role in phytoremediation, microbiology, archaeology, mineral exploration and phytomining*. CAB International: Wallingford, UK, 327–356.

Brooks RR, Trow JM, Veillon J, Jaffré T. 1981. Studies on manganese-hyperaccumulating *Alyxia* species from New Caledonia. *Taxon* **30**:420–423.

Budka D, Mesjasz-Przybyłowicz J, Tylko G, Przybyłowicz WJ. 2005. Freeze-substitution methods for Ni localization and quantitative analysis in *Berkheya coddii* leaves by means of PIXE. *Nuclear Instruments and Methods in Physics Research, Section B: Beam Interactions with Materials and Atoms* **231**:338–344.

Chaney RL. 1983. Plant uptake of inorganic waste. Land treatment of hazardous wastes. In: Parr JE, Marsh PB, Kla JM, eds. *Land treatment of hazardous wastes*. Park Ridge, IL: Noyes Data Corp, 50–76.

Chaney RL, Angle JS, Baker AJM, Li JM. 1998. *Method for phytomining of nickel, cobalt and other metals from soil*. US Patent # 5711784.

Chaney RL, Angle JS, Broadhurst CL, Peters CA, Tappero RV, Sparks DL. 2007. Improved understanding of hyperaccumulation yields commercial phytoextraction and phytomining technologies. *Journal of Environmental Quality* **36**:1429–1443.

Chaney RL, Baker AJ, Morel JL. 2018. The long road to developing agromining/phytomining. In: A. van der Ent *et al.* (eds.), *Agromining: farming for metals*. Mineral Resource Reviews, Springer International Publishing AG, 1–17.

Chaney RL, Baklanov I, Paul A. 2017. Effect of soil volume on Ni hyperaccumulation from serpentine soil by *Alyssum corsicum*. Presented at the 9th International Conference on Serpentine Ecology, Pogradec, Albania (4–9 June).

Currie LA. 1968. Limits for qualitative detection and quantitative determination. Application to radiochemistry. *Analytical Chemistry* **40**:586–593.

DalCorso G, Manara A, Piasentin S, Furini A. 2014. Nutrient metal elements in plants. *Metallomics* **6**:1770–1788.

Doolittle LR. 1986. A semiautomatic algorithm for Rutherford backscattering analysis. *Nuclear Instruments and Methods in Physics Research, Section B: Beam Interactions with Materials and Atoms* **15**:227–231.

Fernando DR, Bakkaus EJ, Perrier N, Baker AJ, Woodrow IE, Batianoff GN, Collins RN. 2006a. Manganese accumulation in the leaf mesophyll of four tree species: a PIXE/EDAX localization study. *The New Phytologist* **171**:751–757.

Fernando DR, Batianoff GN, Baker AJ, Woodrow IE. 2006b. In vivo localization of manganese in the hyperaccumulator *Gossia bidwillii* (Benth.) N. Snow & Guymer (Myrtacea) by cryo-SEM/EDAX. *Plant Cell and Environment* **29**:1012–1020.

Fernando DR, Marshall AT, Forster PI, Hoebee SE, Siegele R. 2013. Multiple metal accumulation within a manganese-specific genus. *American Journal of Botany* **100**:690–700.

Gei V, Echevarria G, Erskine PD, Montarges-Pelletier E, Isnard S, Fogliani B, Jaffre T, Spiers KM, Garrevoet J, van der Ent A. 2020. Soil chemistry, elemental profiles and elemental distribution in nickel hyperaccumulator species from New Caledonia. *Plant and Soil* **457** (1-2), 293–320.

Jaffré T, Brooks RR, Lee J, Reeves RD. 1976. *Sebertia acuminata*: a hyperaccumulator of nickel from New Caledonia. *Science* **193**:579–580.

Kachenko AG, Singh B, Bhatia NP, Siegele R. 2008. Quantitative elemental localisation in leaves and stems of nickel hyperaccumulating shrub *Hybanthus floribundus* subsp. *floribundus* using micro-PIXE spectroscopy. *Nuclear Instruments and Methods in Physics Research, Section B: Beam Interactions with Materials and Atoms* **266**:667–676.

Kersten WJ, Brooks RR, Reeves RD, Jaffré A. 1980. Nature of nickel complexes in *Psychotria douarrei* and other nickel-accumulating plants. *Phytochemistry* **19**:1963–1965.

Küpper H, Lombi E, Zhao FJ, Wieshammer G, McGrath SP. 2001. Cellular compartmentation of nickel in the hyperaccumulators *Alyssum lesbiacum*, *Alyssum bertolonii* and *Thlaspi goesingense*. *Journal of Experimental Botany* **52**:2291–2300.

Lee J, Reeves RD, Brooks RR, Jaffré T. 1977. Isolation and identification of a citrato-complex of nickel from nickel-accumulating plants. *Phytochemistry* **16**:1503–1505.

Lee J, Reeves RD, Brooks RR, Jaffré T. 1978. The relation between nickel and citric acid in some nickel-accumulating plants. *Phytochemistry* **17**:1033–1035.

McNear DH Jr, Peltier E, Everhart J, Chaney RL, Sutton S, Newville M, Rivers M, Sparks DL. 2005. Application of quantitative fluorescence and absorption-edge computed microtomography to image metal compartmentalization in *Alyssum murale*. *Environmental Science & Technology* **39**:2210–2218.

Mesjasz-Przybyłowicz J, Balkwill K, Przybyłowicz WJ, Annegarn HJ. 1994. Proton microprobe and X-ray fluorescence investigations of nickel distribution in serpentine flora from South Africa. *Nuclear Instruments and Methods in Physics Research, Section B: Beam Interactions with Materials and Atoms* **89**:208–212.

Mesjasz-Przybyłowicz J, Balkwill K, Przybyłowicz W, Annegarn H, Rama D. 1996. Similarity of nickel distribution in leaf tissue of two distantly related hyperaccumulating species. In: van der Maesen LJG, van de Burgt XM, van Medenbach de Roy JM, eds. *"The biodiversity of African plants", Proceedings XIVth AETFAT Congress*. Dordrecht: Kluwer Academic Publishers, 331–335.

Mesjasz-Przybyłowicz J, Barnabas A, Przybyłowicz W. 2007. Comparison of cytology and distribution of nickel in roots of Ni-hyperaccumulating and non-hyperaccumulating genotypes of *Senecio coronatus*. *Plant and Soil* **293**:61–78.

Mesjasz-Przybyłowicz J, Barnabas A, Przybyłowicz W. 2016a. Exceptionally high Ni concentration in phloem of roots of nickel hyperaccumulating *Berkheya zeyheri* subsp. *rehmannii* var. *rogersiana*. *Microscopy and Microanalysis* **22**:1028–1029.

Mesjasz-Przybyłowicz J, Przybyłowicz W. 2011. PIXE and metal hyperaccumulation: from soil to plants and insects. *X-Ray Spectrometry* **40**:181–185.

Mesjasz-Przybyłowicz J, Przybyłowicz WJ. 2020. Ecophysiology of nickel hyperaccumulating plants from South Africa - from ultramafic soil and mycorrhiza to plants and insects. *Metallomics* **12**:1018–1035.

Mesjasz-Przybyłowicz J, Przybyłowicz W, Barnabas A, van der Ent A. 2016b. Extreme nickel hyperaccumulation in the vascular tracts of the tree *Phyllanthus balgooyi* from Borneo. *The New Phytologist* **209**:1513–1526.

Mesjasz-Przybyłowicz J, Przybyłowicz WJ, Prozesky VM, Pineda CA. 1997. Quantitative micro-PIXE comparison of elemental distribution in Ni-hyperaccumulating and non-accumulating genotypes of *Senecio coronatus*. *Nuclear Instruments and Methods in Physics Research, Section B: Beam Interactions with Materials and Atoms* **130**:368–373.

Mesjasz-Przybyłowicz J, Przybyłowicz W, Rama D, Pineda C. 2001. Elemental distribution in *Senecio anomalochrous*, a Ni hyperaccumulator from South Africa. *South African Journal of Science* **97**:593–595.

Morgan JB, Connolly EL. 2013. Plant-soil interactions: nutrient uptake. *Nature Educational Knowledge* **4**:2.

Orłowska E, Przybyłowicz W, Orłowski D, Mongwaketsi NP, Turnau K, Mesjasz-Przybyłowicz J. 2013. Mycorrhizal colonization affects the elemental distribution in roots of Ni-hyperaccumulator *Berkheya coddii* Roessler. *Environmental Pollution* **175**: 100–109.

Paul ALD, Gei V, Isnard S, Fogliani B, Echevarria G, Erskine PD, Jaffré T, Munzinger J, van der Ent A. 2020. Nickel hyperaccumulation in New Caledonian *Hybanthus* (Violaceae) and occurrence of nickel-rich phloem in *Hybanthus austrocaledonicus*. *Annals of Botany* **126**:905–914.

Pilon-Smits EA, Quinn CF, Tapken W, Malagoli M, Schiavon M. 2009. Physiological functions of beneficial elements. *Current Opinion in Plant Biology* **12**:267–274.

Prozesky V, Przybyłowicz W, Van Achterbergh E, Churms C, Pineda C, Springhorn K, Pilcher J, Ryan C, Kritzinger J, Schmitt H. 1995. The NAC nuclear microprobe facility. *Nuclear Instruments and Methods in Physics Research, Section B: Beam Interactions with Materials and Atoms* **104**:36–42.

Przybyłowicz W, Mesjasz-Przybyłowicz J, Migula P, Nakonieczny M, Augustyniak M, Tarnawska M, Turnau K, Ryszka P, Orłowska E, Zubek S. 2005. Micro-PIXE in ecophysiology. *X-Ray Spectrometry* **34**:285–289.

Przybyłowicz W, Mesjasz-Przybyłowicz J, Pineda C, Churms C, Springhorn K, Prozesky V. 1999. Biological applications of the NAC nuclear microprobe. *X-Ray Spectrometry* **28**:237–243.

Reeves R. 2006. Hyperaccumulation of trace elements by plants. In: Morel J-L, Echevarria G, Goncharova N, eds. Proceedings of the NATO Advanced Study Institute, Třešť Castle, Czech Republic, 18–30 August 2002. *Phytoremediation of metal-contaminated soils. NATO Science Series: IV: Earth and Environmental Sciences*, vol. **68**. Berlin: Springer, 25–52.

Reeves RD. 2003. Tropical hyperaccumulators of metals and their potential for phytoextraction. *Plant and Soil* **249**:57–65.

Reeves RD, Baker AJM, Jaffré T, Erskine PD, Echevarria G, van der Ent A. 2017. A global database for plants that hyperaccumulate metal and metalloid trace elements. *The New Phytologist* **218**:407–411.

Robinson BH, Lombi E, Zhao FJ, McGrath SP. 2003. Uptake and distribution of nickel and other metals in the hyperaccumulator *Berkheya coddii*. *The New Phytologist* **158**:279–285.

Rowley S, Cardon G, Black B. 2012. Macronutrient management for Utah Orchards. USU Extension Publication Horticulture/Fruit/201-01pr.

Ryan C. 2000. Quantitative trace element imaging using PIXE and the nuclear microprobe. *International Journal of Imaging Systems and Technology* **11**:219–230.

Ryan C, Cousens D, Sie S, Griffin W. 1990a. Quantitative analysis of PIXE spectra in geoscience applications. *Nuclear Instruments and Methods in Physics Research, Section B: Beam Interactions with Materials and Atoms* **49**:271–276.

Ryan C, Cousens D, Sie S, Griffin W, Suter G, Clayton E. 1990b. Quantitative PIXE microanalysis of geological matemal using the CSIRO proton microprobe. *Nuclear Instruments and Methods in Physics Research, Section B: Beam Interactions with Materials and Atoms* **47**:55–71.

Ryan C, Jamieson D. 1993. Dynamic analysis: on-line quantitative PIXE microanalysis and its use in overlap-resolved elemental mapping. *Nuclear Instruments and Methods in Physics Research, Section B: Beam Interactions with Materials and Atoms* **77**:203–214.

Ryan C, Jamieson D, Churms C, Pilcher J. 1995. A new method for on-line true-elemental imaging using PIXE and the proton microprobe. *Nuclear Instruments and Methods in Physics Research, Section B: Beam Interactions with Materials and Atoms* **104**:157–165.

Severne BC. 1974. Nickel accumulation by *Hybanthus floribundus*. *Nature* **248**:807–808.

Shanker AK, Venkateswarlu B. 2011. *Abiotic stress in plants-mechanisms and adaptations*. Tech Publisher, Croatia 1–428.

Tappero R, Peltier E, Gräfe M, Heidel K, Ginder-Vogel M, Livi KJ, Rivers ML, Marcus MA, Chaney RL, Sparks DL. 2007. Hyperaccumulator *Alyssum murale* relies on a different metal storage mechanism for cobalt than for nickel. *The New Phytologist* **175**:641–654.

van Achterbergh E, Ryan CG, Gurney JJ, Le Roex AP. 1995. PIXE profiling, imaging and analysis using the NAC proton microprobe: unraveling mantle eclogites. *Nuclear Instruments and Methods in Physics Research, Section B: Beam Interactions with Materials and Atoms* **104**:415–426.

van der Ent A, Baker AJM, Reeves RD, Pollard AJ, Schat H. 2013a. Hyperaccumulators of metal and metalloid trace elements: facts and fiction. *Plant and Soil* **362**:319–334.

van der Ent A, Baker A, Van Balgooy M, Tjoa A. 2013b. Ultramafic nickel laterites in Indonesia (Sulawesi, Halmahera): mining, nickel hyperaccumulators and opportunities for phytomining. *Journal of Geochemical Exploration* **128**:72–79.

van der Ent A, Callahan DL, Noller BN, Mesjasz-Przybyłowicz J, Przybyłowicz WJ, Barnabas A, Harris HH. 2017a. Nickel biopathways in tropical nickel hyperaccumulating trees from Sabah (Malaysia). *Scientific Reports* **7**:41861.

van der Ent A, Cardace D, Tibbett M, Echevarria G. 2017b. Ecological implications of pedogenesis and geochemistry of ultramafic soils in Kinabalu Park (Malaysia). *Catena* **160**:154–169.

van der Ent A, de Jonge MD, Mak R, Mesjasz-Przybyłowicz J, Przybyłowicz WJ, Barnabas AD, Harris HH. 2020. X-ray fluorescence elemental mapping of roots, stems and leaves of the nickel hyperaccumulators *Rinorea* cf. *bengalensis* and *Rinorea* cf. *javanica* (Violaceae) from Sabah (Malaysia), Borneo. *Plant and Soil* **448**:15–36.

van der Ent A, Echevarria G, Baker AJM, Morel JL. 2017c. *Agromining: extracting unconventional resources from plants. Mineral Resource Reviews Series*. Springer Nature, 594 pp.

van der Ent A, Erskine PD, Mulligan DR, Repin R, Karim R. 2016. Vegetation on ultramafic edaphic islands in Kinabalu Park (Sabah, Malaysia) in relation to soil chemistry and altitude. *Plant and Soil* **403**:77–101.

van der Ent A, Erskine P, Sumail S. 2015a. Ecology of nickel hyperaccumulator plants from ultramafic soils in Sabah (Malaysia). *Chemoecology* **25**:243–259.

van der Ent A, Mak R, de Jonge MD, Harris HH. 2018. Simultaneous hyperaccumulation of nickel and cobalt in the tree *Glochidion* cf. *sericeum* (Phyllanthaceae): elemental distribution and chemical speciation. *Scientific Reports* **8**:9683.

van der Ent A, Mulligan D. 2015. Multi-element concentrations in plant parts and fluids of Malaysian nickel hyperaccumulator plants and

some economic and ecological considerations. *Journal of Chemical Ecology* **41**:396–408.

van der Ent A, Mulligan DR, Repin R, Erskine PD. 2019a. Foliar elemental profiles in the ultramafic flora of Kinabalu Park (Sabah, Malaysia). *Ecological Research* **33**:659–674.

van der Ent A, Ocenar A, Tisserand R, Sugau JB, Erskine PD, Echevarria G. 2019b. Herbarium X-ray fluorescence screening for nickel, cobalt and manganese hyperaccumulation in the flora of Sabah (Malaysia, Borneo Island). *Journal of Geochemical Exploration* **202**:49–58.

van der Ent A, Repin R, Sugau J, Wong KM. 2014. *The ultramafic flora of Sabah: an introduction to the plant diversity on ultramafic soils*. Kota Kinabalu, Malaysia: Natural History Publications (Borneo); Sabah Parks.

van der Ent A, van Balgooy M, van Welzen P. 2015b. *Actephila alanbakeri* (Phyllanthaceae): a new nickel hyperaccumulating plant species from localised ultramafic outcrops in Sabah (Malaysia). *Botanical Studies* **57**:6.